

# Microfabricated rubber microscope using soft solid immersion lenses

Yann Gambin, Olivier Legrand, and Stephen R. Quake<sup>a)</sup>

Department of Applied Physics, California Institute of Technology, Pasadena, California 91125

(Received 5 November 2005; accepted 6 March 2006; published online 24 April 2006)

We show here a technique of soft lithography to microfabricate efficient solid immersion lenses (SIL) out of rubber elastomers. The light collection efficiency of a lens system is described by its numerical aperture (NA), and is critical for applications as epifluorescence microscopy [B. Herman, *Fluorescence Microscopy* (BIOS Scientific, Oxford/Springer, United Kingdom, 1998)]. While most simple lens systems have numerical apertures less than 1, the lenses described here have  $NA = 1.25$ . Better performance can be engineered though the use of compound designs; we used this principle to make compound solid immersion lenses ( $NA = 1.32$ ). An important application of these lenses will be as integrated optics for microfluidic devices. We incorporated them into a handheld rubber microscope for microfluidic flow cytometry and imaged single *E. Coli* cells by fluorescence. © 2006 American Institute of Physics. [DOI: 10.1063/1.2194477]

The simplest possible optical lenses are spherical, and there are two cuts of a solid sphere that yield aberration free imaging.<sup>1</sup> If one cuts through the middle of the sphere, the resulting hemispherical lens will enhance the numerical aperture of an optical system by  $n$ , the index of refraction of the lens material. If one cuts a slice a distance  $R + R/n$  from the top of a sphere of radius  $R$ , the resulting lens will enhance numerical aperture by  $n^2$ , a significant improvement which has allowed the development of optical devices with numerical apertures greater than 1. Kino and co-workers have explored the use of these ball lenses, which they termed solid immersion lenses (SIL).<sup>2–4</sup>

An important limitation to SILs that has hampered their widespread adoption is that they are difficult to manufacture. Although there has been some progress,<sup>5</sup> the high performance “Weierstrass” SIL still requires hand grinding and polishing due to its highly undercut features. We applied the techniques of soft lithography to make molded SILs out of the elastomer polydimethylsiloxane (PDMS) ( $n = 1.41$ ). Soft lithography has been previously used to make a variety of fluidic, mechanical, electronic, and optical devices.<sup>6,7</sup> Optical devices demonstrated to date include a blazed grating<sup>8</sup> and lasing cavity.<sup>9</sup> An elastomeric mold is the ideal fabrication technique for a SIL, because the mold can stretch and allow the undercut features to be removed without damage to the lens or the mold.

Large SILs can be made using a simple molding process. Stainless steel ball bearings with diameters ranging from 0.5 to 2 cm were used as positive molds. The flexible elastomer PDMS was used both for the negative molds and for the lenses themselves. Attempts to mold smaller lenses that would be compatible with microfabricated devices run into a fundamental problem; the surface tension of the PDMS causes it to creep on the positive mold. We controlled this phenomenon by partially curing the PDMS before using it; the reticulation of polymer chains changes the viscosity of the uncured PDMS in a controllable manner. By heating a thin layer of PDMS for 2 or 3 min at 80 °C, it is possible to

obtain exactly the desired depth of the mold for the SIL. This process can be calibrated precisely, as shown in Fig. 1. The depth of the mold is determined by measuring a SIL made from this mold. The results are highly reproducible, with a precision of 20  $\mu\text{m}$ . To create the mold of the smaller SIL we used a 150  $\mu\text{m}$  radius microsphere (ruby ball lenses, Edmund industrial optics, see Fig. 2).

In order to characterize the performance of the SILs, we measured their numerical apertures using fluorescence microscopy. A simple microscope was constructed such that the amount of fluorescence from a latex bead could be measured, with and without the SIL. For most experiments a blue light-emitting diode (LED) (Luxeon Star/C) was used for excitation, but on occasion a higher power argon laser (Uniphase) was used. The blue LED is in the focal point of a collimating lens (diameter  $l = 1.9$  cm and focal length  $f = 3$  cm), while the laser is beam expanded by a telescope (lens focal lengths  $= -2$  and 4 cm). The excitation illumination is filtered by a bandpass filter (465–495 nm), and is reflected by a dichroic filter (505 nm) toward a lens (diameter  $l = 1.9$  cm and focal length  $f = 1.15$  cm) that focuses the light on the SIL. This

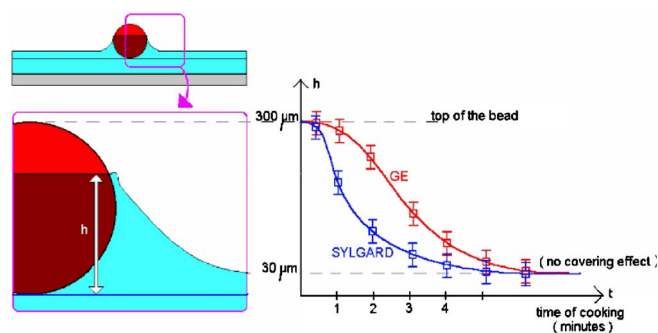


FIG. 1. (Color online) The height  $h$  of the mold can be calibrated for different times of precuring the PDMS. The left figure shows a schematic diagram illustrating how the height of the mold is measured. The graph on the right shows that data are plotted in blue for the experiments made with General Electric RTV, and in red for the lens created with Sylgard PDMS. It allows a precise estimation of the time of curing, at 80 °C, needed to obtain a certain depth of the mold. The calibration curve determines the time of cooking to create the right depth of the mold: to have exactly  $h = R(1 + 1/n)$ , one needs to bake less than 1 min for Sylgard and 2 min and 20 s for RTV.

<sup>a)</sup> Author to whom correspondence should be addressed; present address: Howard Hughes Medical Institute and Department of Bioengineering, Stanford University, Stanford, CA 94305; electronic mail: quake@stanford.edu

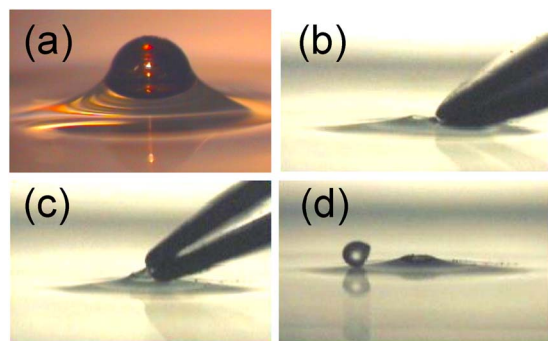


FIG. 2. (Color online) *SIL fabrication procedure*. To make a first layer of RTV, fresh RTV is poured on a cover slip. After spinning at 700 rpm for 1 min, this layer is cured at 80 °C for 30 min. Another layer 30 μm thick is created with repeating the pouring and spinning on the same sample. This layer is precured according to the calibration curve in Fig. 1(a). (a) 300 μm diameter balls are then placed in the middle of the cover slip, which is replaced in the oven and cooked for 45 min. (b) The bead can then be removed from the mold, even though the diameter of the bead is larger than the aperture of the mold, because of the elasticity of the PDMS. The sample is then exposed to an oxygen plasma for 2 min, which prevents the mold from sticking to a new layer of PDMS. (c) An excess of silicon is poured on top of the mold, after which the sample is placed in vacuum. After that, the cover slip is spun at 700 rpm for 1 min, to create a flat surface, with the right thickness for the lens. The final curing is 45 min at 80 °C. (d) The SIL is then extracted from its mold. Note that this technique is easily used to produce many SILs on the same mold.

lens is also used for collection and has been chosen so that the initial numerical aperture of the microscope (without the SIL) is  $NA=0.63$ . The SIL is put over a PDMS chip in which fluorescent beads (Interfacial Dynamics Corporation 2-FY-1K.2, diameter of 5 μm, concentration of  $2 \times 10^8$  beads/ml) are flowing inside a microchannel (1 cm length, 20 μm width, and 5 μm deep). The collected fluorescence is filtered by an emission filter (515–555 nm) and is focused by a lens ( $f=17.5$  cm) onto a charge-coupled device (CCD) camera (Philips Image Sensor Module FTM 800). The SIL increases both the size and the intensity of the spot (Fig. 3). We varied the illumination intensity in order to demonstrate that the

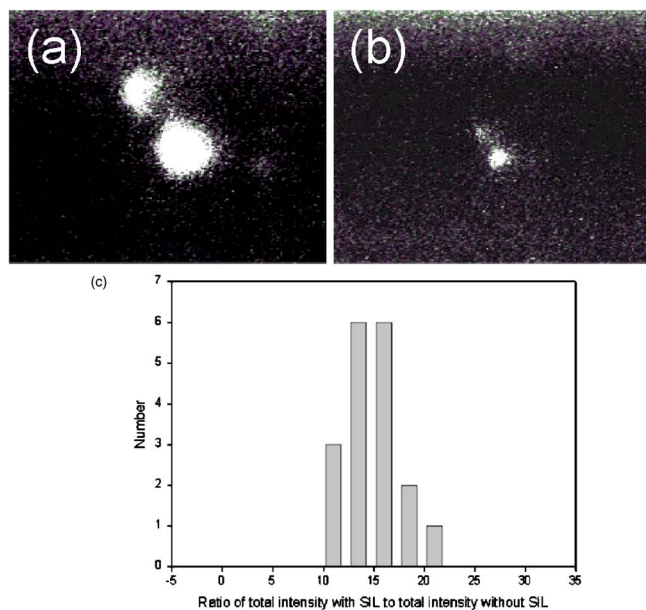


FIG. 3. (Color online) Images of the same fluorescent beads taken (a) with and (b) without SIL. (c) Analysis of the image intensities of many such images shows that the SIL increases measured intensity by a factor of 15.

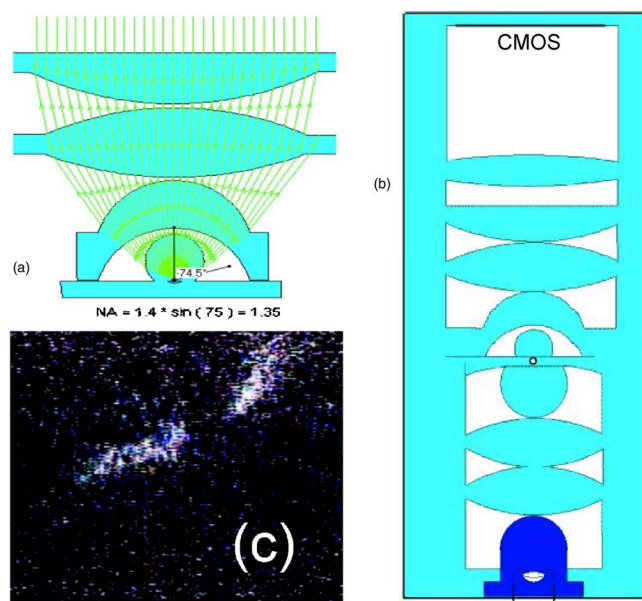


FIG. 4. (Color online) (a) The compound SILs. To create the mold for the double curve SIL we used a 395 μm radius microsphere (Ruby ball lenses, Edmund Industrial Optics). (b) Schematic diagrams of the elastomeric microscope. The microscope incorporates a microfluidic chip in the focal plane so that fluorescent *E. Coli* can be imaged and is only 10 cm long, including the CMOS camera that is used for video imaging. The eight lenses of the microscope are all made with PDMS. (c) Image from the microscope's camera of two *E. Coli* cells expressing green fluorescent protein. Without the SIL, fluorescence from the cells is not visible.

efficiency of the SIL does not depend on the brightness of the objects. A wide range of SIL sizes were used for these experiments, from a 2 mm to a 395 μm radius SIL; all gave similar results.

The ratio of the total intensity collected, with and without the SIL, is related to the respective numerical apertures, with and without the SIL,

$$\frac{NA_{\text{with SIL}}}{NA_{\text{without SIL}}} = \left( \frac{I_{\text{with SIL}}}{I_{\text{without SIL}}} \right)^{1/4}. \quad (1)$$

The average ratio of the two intensities is  $15.35 \pm 0.53$ , as shown in the histogram in Fig. 3(c). The initial numerical aperture of the microscope without the SIL is 0.63, so the measured numerical aperture of the SIL is  $NA=1.25 \pm 0.02$ . This result is in good agreement with the theoretical prediction of 1.26.

The performance of a lens can be improved by adding several elements; the highest performance microscope objectives have as many as 20 elements to improve light collection ability while correction for various optical aberrations. Ray tracing diagrams suggest that one can improve the light collection ability of a SIL by creating the compound element shown in Fig. 4(a). That particular design should improve light collection ability to a NA of 1.32 (prediction by RAY-TRACE software), close to the index of refraction of PDMS.

A powerful future application for SILs is as integrated optics in microfluidic devices and DNA chip applications. These applications often use optical, usually fluorescent, readout techniques and benefit from the use of high numerical aperture optics. In a monolithic, integrated device there are no interface problems that interfere with the ability of the SIL to collect light at its full theoretical numerical aperture. SILs fabricated by soft lithography have the further advantage of being easily integrated with other microfluidic components.

tage that they can be easily integrated into elastomeric microfluidic devices. Multilayer soft lithography has been previously used to create integrated microvalves and pumps,<sup>10</sup> which in turn have been used to make integrated microfluidic cell sorters<sup>11</sup> and DNA amplification devices.<sup>12</sup>

We fabricated the compound SILs and other elastomeric optics shown in Fig. 4(b) by simple molding procedures to make a self-contained microfluidic microscope and integrated them in a microfluidic flow cytometer; the only components not made of rubber are the mounting frame, the light source, the dielectric filter to separate fluorescent excitation from emission and a complementary metal-oxide semiconductor (CMOS) sensor record the image. The SIL has a radius of 150  $\mu\text{m}$  and is mounted directly on the microfluidic flow cytometry chip, also made of PDMS. The total linear size of the microscope is about 10 cm. This integrated optical flow cytometer was used to image individual *E. Coli* cells expressing green fluorescent protein with good signal to noise ratio, using a lightweight and low-cost blue LED as a fluorescent excitation source. The cells were suspended into phosphate buffer (4.3 mM  $\text{Na}_2\text{HPO}_4 \cdot 7\text{H}_2\text{O}$  and 1.4 mM  $\text{KH}_2\text{PO}_4$ ) containing 10  $\mu\text{M}$  sodium dodecyl sulphate and diluted to a concentration of 109 cells/ml. In the absence of the compound SIL the microscope is unable to detect any cells; even with increased power from the LED, no fluorescent signal can be seen. With the compound SIL, the cells can be easily imaged, as shown in Fig. 4(c). Typically, the cells are 2  $\mu\text{m}$  long and 1  $\mu\text{m}$  large. Brightfield images show that using the SIL increases the magnification by about a factor of 2, close to the expected value.

In conclusion, soft lithography can be used to fabricate high performance optics. The highly undercut morphology of

the SIL component makes it difficult, if not impossible, to fabricate using conventional microfabrication techniques. These optics can easily be integrated into complex devices (such as the handheld microfluidic flow cytometer) and single use chips for healthcare diagnostic (thanks to the PDMS low cost). It is also possible that such optics will find use in other high performance applications such as photonics and telecommunications.

The authors would like to thank Todd Thorsen and Markus Enzelberger for helpful discussions. This work was supported by the DARPA Chips program and the US National Science Foundation.

<sup>1</sup>M. Born and E. Wolf, *Principles of Optics* (Cambridge University Press, Cambridge, United Kingdom, 1999).

<sup>2</sup>S. M. Mansfield and G. S. Kino, *Appl. Phys. Lett.* **57**, 2615 (1990).

<sup>3</sup>S. M. Mansfield, W. R. Stundenmund, G. S. Kino, and K. Osato, *Opt. Lett.* **18**, 305 (1993).

<sup>4</sup>B. D. Terris, H. J. Mamin, D. Rugar, W. R. Stundenmund, and G. S. Kino, *Appl. Phys. Lett.* **65**, 388 (1994).

<sup>5</sup>D. A. Fletcher, K. B. Crozier, K. W. Guarini, S. C. Minne, G. S. Kino, C. F. Quate, and K. E. Goodson, *J. Microelectromech. Syst.* **10**, 450 (2001).

<sup>6</sup>Y. N. Xia and G. M. Whitesides, *Angew. Chem., Int. Ed.* **37**, 550 (1998).

<sup>7</sup>S. R. Quake and A. Scherer, *Science* **290**, 1536 (2000).

<sup>8</sup>Y. N. Xia, E. Kim, X. Zia, J. A. Rogers, M. Prentiss, and G. M. Whitesides, *Science* **273**, 347 (1996).

<sup>9</sup>P. D. Yang, G. Wirsberger, H. C. Huang, S. R. Cordero, M. D. McGehee, B. Scott, T. Deng, G. M. Whitesides, B. F. Chmelka, S. K. Buratto, and G. D. Stucky, *Science* **287**, 465 (2000).

<sup>10</sup>M. A. Unger, H. P. Chou, T. Thorsen, A. Scherer, and S. R. Quake, *Science* **288**, 113 (2000).

<sup>11</sup>A. Y. Fu, H. P. Chou, C. Spence, F. H. Arnold, and S. R. Quake, *Anal. Chem.* **74**, 2451 (2002).

<sup>12</sup>J. Liu, M. Enzelberger, and S. R. Quake, *Electrophoresis* **23**, 1531 (2002).